Fracture Mechanics of Concrete Structures, de Borst et al (eds) © 2001 Swets & Zeitlinger, Lisse, ISBN 90 2651 825 0

Softening properties of concrete under biaxial loading

S.Ishiguro
Faculty of Bioresources, Mie University, Tsu, Mie, Japan

ABSTRACT: The load-displacement curves for concrete under biaxial (tension-compression) loading conditions were measured using rectangular notched specimens and wedge splitting procedures. The polylinear inverse analysis method was used to determine the tension softening diagrams from the load-displacement curves. The observed differences in the biaxial fracture behavior between natural and crushed aggregate concrete are analyzed and discussed. The influences of compressive loading on softening properties, such as the shape of the curve or tensile strength, were also investigated from the analytical results.

1 INTRODUCTION

Massive concrete structures are generally in a multi-axial stress state when cracks form and propagate. To reproduce this condition, Tschegg et al. (1992) developed a wedge splitting test method, which allows biaxial tensile-compressive loading. They used the test method to evaluate the fracture parameters of concrete made with aggregates of different maximum sizes. Bilinear softening diagrams of the concrete were also determined by SOFTFIT, which is a widely used data fit program. From the experimental and analytical results, a fracture model was developed that explains fracture behavior under biaxial tensile-compressive loading. Tschegg et al. (1995) then developed a new wedge splitting test method using a hydraulic pressure device. Biaxial fracture parameters of concrete made with either natural or crushed gravel and under different storage conditions were evaluated using this method. Tschegg et al. discussed many interesting aspects of fracture testing techniques and devices. In particular, they considered the load-displacement curves, specific fracture energy, and notch tensile strength of concrete under biaxial loading.

The tension softening diagram is a very important fracture parameter in concrete, as well as the specific fracture energy. Therefore, this study focused on evaluating the tension softening properties of concrete under combined tensile-compressive loading. The softening diagrams of natural and crushed aggregate concrete were characterized using polylinear inverse analysis, and the fracture properties of the two types of concrete were compared.

2 EXPERIMENTAL PROCEDURE

2.1 *Specimens*

A concrete specimen, illustrated in Figure 1, was used for uniaxial and biaxial fracture tests. A starter notch (2 mm wide) was cut in the top of the specimen with a stone saw shortly before testing. Biaxial loading (compressive force *Fc*; tension force *Fh*) was

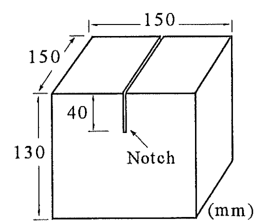

Figure 1. Size and shape of the specimen used for uniaxial and biaxial fracture tests

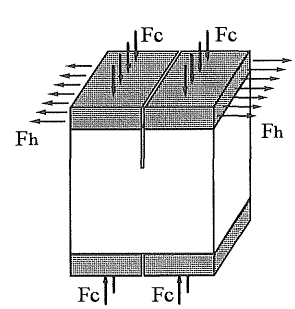

Figure 2. Biaxial loading state of the specimen

applied to the single-edge notched concrete specimen as shown in Figure 2.

2.2 *Biaxial loading system*

A schematic of the wedge-splitting test method, developed by Tschegg et al. (1991, 1995), is given in Figure 3. The single-edge notched specimen is placed on a narrow linear support in a compression-testing machine. A wedge splitting apparatus, comprised of a wedge and load transmission slabs, is placed into a compressive loading unit (see Figure 3(b)) consisting of two frames that can be completely separated. These frames are made up of tensile bars and flexurally rigid bars, which are connected to the elevating frame (see Figure 3(c)) at the top of each upper beam. The frames can move horizontally when the wedge splits the concrete specimen. The wedge, starter notch, and linear support are vertically aligned, which allows the load to be transmitted directly from the testing machine to the specimen without producing additional lateral loads or moments.

The wedge transmits a force (*Fm*) from the testing machine to the specimen. This force is transformed by the slender wedge into a large horizontal component (*Fh*) and a small vertical component (*Fv*), which are then applied to the specimen (see Figure 3(a)). The large horizontal component splits the specimen in a manner similar to a bending test. A load cell in the testing machine measures the total force (*Fm*). Since the wedge angle (α) is known, the horizontal component (*Fh*) is calculated as follows.

$$Fh = \frac{Fm}{2\tan(\alpha/2)} \tag{1}$$

A compressive force (*Fc*) is applied to the specimen using a hydraulic system. Three hydraulic cylinders are mounted on each upper beam (see Figure 3(b)); the six cylinders in total generate a maximum force of 400 kN.

The displacement (δ) of the specimen, referred to as the Crack Mouth Opening Displacement (CMOD), is measured at each end of the notch using a 5-mm

Table 1. Properties of concrete

	NG-Concrete	CG-Concrete
Cement (kg/m^3)	280	280
Water (kg/m^3)	168	168
Water:cement ratio (w/c)	0.6	0.6
Type of coarse aggregate	Natural gravel	Crushed gravel
Maximum size of aggregate (mm)	20	20
Compressive strength (MPa)	24.7	27.7
Tensile strength (MPa)	2.30	2.59
Modulus of elasticity (GPa)	24.9	30.7

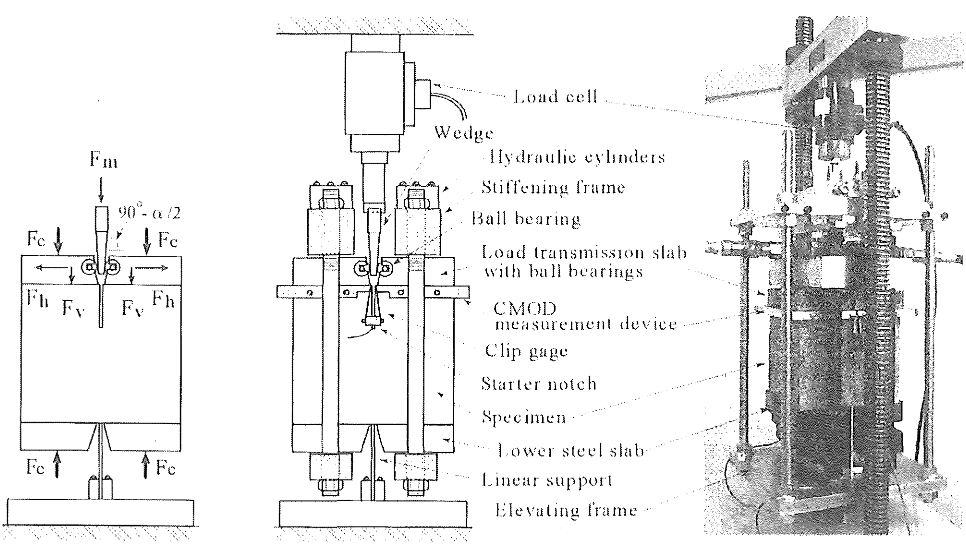

(a) (b) (c)

Figure 3. Wedge-splitting method (a) biaxial loading state, (b) view of the biaxial load system and (c) experimental set-up. The wedge loading devices are based on the techniques developed by Tschegg et al. (1995)

clip gauge. The mean values of the two δ measurements are used to reduce the uncertainty.

2.3 *Material and experimental details*

Concretes with natural gravel (NG) and crushed gravel (CG) were tested. The mix ratio of the concretes, compressive and tensile strengths, and modulus of elasticity are listed in Table 1.

The specimens were allowed to harden for 24 hours after casting, before being removed from their molds and stored in water for 28 days before testing.

The concrete specimens were tested under different loading conditions (normalized compressive loading stages σ_1/fc = 0.0, 0.15, 0.30, 0.45, and 0.60, where σ_1 is the compressive stress and fc is the compressive strength of the concrete). Tests were performed using a mechanical compression-testing machine with a load capacity of 9.8 kN. The crosshead velocity for each test was 1 mm/min. All testing was performed on four identical specimens of each material to obtain sufficient data for a statistical evaluation.

In the uniaxial fracture test (σ_1/fc = 0.0), an adhesive was used to stick the upper load transmission slabs to the concrete specimen shortly before testing. The shape and size of the specimens used were the same for the uniaxial and biaxial fracture tests.

The force (Fm) and the two end displacements ($\delta 1$ and $\delta 2$) were recorded by an electronic data logger at 1.0-second intervals. The data were then analyzed to produce a load-displacement curve (Fh-CMOD curve).

2.4 *Evaluation of test results*

The measured load-displacement curves of NG and CG concrete are given in Figure 4 for compressive loading stages of σ_1/fc = 0.0, 0.30, and 0.60. The load-displacement graph characterizes the fracture properties of the concrete. In this study, fracture parameters, such as the specific fracture energy (Gf), notch tensile strength (σ_{2max}), and the tension softening diagram, are derived from the experimental results.

The area under the load-displacement curve represents the energy needed to fracture the specimen (fracture energy). The specific fracture energy (Gf) is a measure of the crack growth resistance of the material, and is defined as the ratio of fracture energy to fracture area, normal to the wedge penetration direction.

The maximum load in the load-displacement diagram (F_{hmax}) may be used to calculate the conventional notch tensile strength (σ_{2max}), as described by Tschegg et al. (1995). The notch tensile strength is calculated as follows:

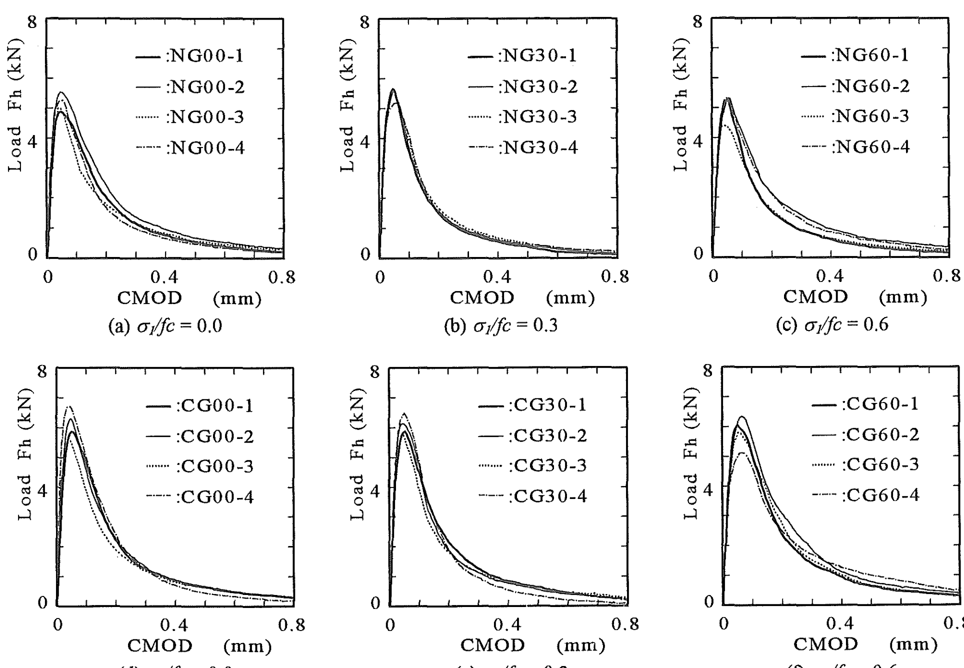

(a) σ_1/fc = 0.0 (b) σ_1/fc = 0.3 (c) σ_1/fc = 0.6

(d) σ_1/fc = 0.0 (e) σ_1/fc = 0.3 (f) σ_1/fc = 0.6

Figure 4. Measured load (Fh)-displacement (CMOD) curves

$$\sigma_{2\max} = \frac{M}{W_{lig}} + \frac{F_{h\max}}{A_{lig}} \quad (2)$$

$$M = y \cdot F_{h\max} \quad (3)$$

$$W_{lig} = \frac{B_{lig} + H_{lig}^2}{6} \quad (4)$$

$$A_{lig} = B_{lig} \cdot H_{lig} \quad (5)$$

where M is the maximum moment, y is the distance from the axis of force application to the center of the ligament area, W_{lig} is the maximum moment of resistance referred to the notch root, and A_{lig} is the area of the plane projection of the ligament area.

The tension softening diagram characterizes the relation between the crack width and the tensile stress of the concrete, and is useful for evaluating the toughness of new materials and fiber-reinforced concrete. The evaluation methods of tension softening diagram are classified into some groups (Nakamura et al. 1999). In this study, polylinear inverse analysis was used to determine the exact shape of the tension softening diagram from the measured load-displacement curve (see Chapter 3).

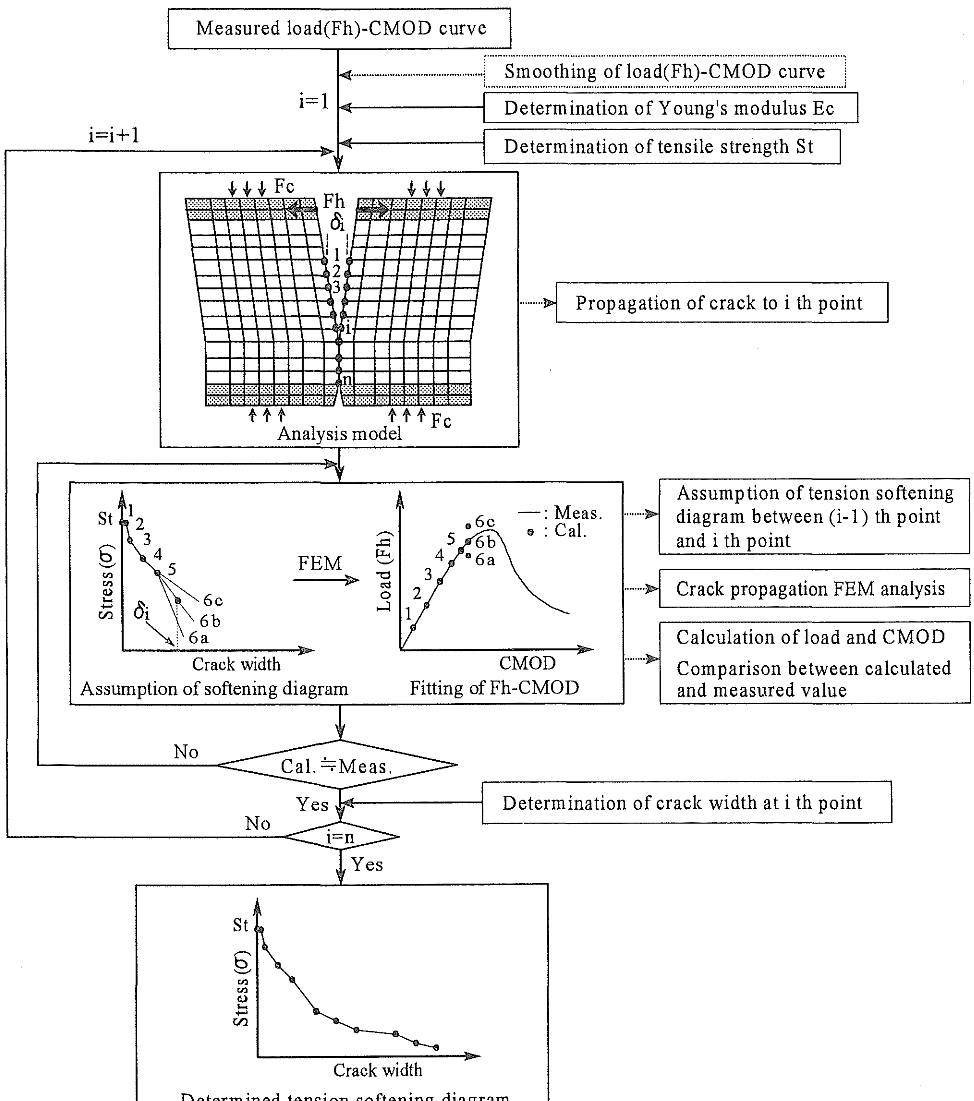

Figure 5. Flow diagram of polylinear inverse analysis method

3 TENSION SOFTENING DIAGRAM ANALYSIS

In order to characterize the fracture behavior of concrete fully, the strain softening behavior must be determined from a tension softening diagram. This study used a polylinear inverse analysis of the experimentally measured *Fh*-CMOD curves. The polylinear inverse analysis was based on the finite element method applied using the fictitious crack model (Uchida et al. 1995, Kitsutaka et al. 1998), and was developed specifically for biaxial loading conditions (Ishiguro, 1997). A flow diagram of the polylinear inverse analysis method is provided in Figure 5.

The characteristic values of the polylinear softening diagram are obtained using an iterative best-fit procedure to match the calculated and measured load-displacement curves. A *Fhcal/Fhmeas* ratio between 0.99 and 1.01 (±1%) was used as the tolerance for the fitting procedure.

4 RESULTS AND DISCUSSION

The specific fracture energy (*Gf*) and notch tensile strength (σ_{2max}) of the concrete specimens were determined from the test results. Figure 6 shows the influence of the compressive stress σ_1 on the specific fracture energy *Gf*. Both decrease and increase in the specific fracture energy under increasing compressive stress was observed. The behavior of the specific fracture energy under biaxial loading agrees with behavior reported in the literature (Tschegg et al., 1995) for similar concrete.

The relationship between the notch tensile strength σ_{2max} and compressive stress σ_1 is plotted in Figure 7 for NG and CG concrete. The notch tensile strengths for loads up to σ_1/fc = 0.6 remain almost constant. Both the notch tensile strength and specific fracture energy are higher for CG concrete than for NG concrete. Comparing the fracture energy *Gf* of NG concrete for different compressive loading stages to that of CG concretes yields the following values:

Gf (CG00) / *Gf* (NG00) = 1.10
Gf (CG15) / *Gf* (NG15) = 1.41
Gf (CG30) / *Gf* (NG30) = 1.18
Gf (CG45) / *Gf* (NG45) = 1.06
Gf (CG60) / *Gf* (NG60) = 1.38

The calculated Young's modulus (*Ec*) of NG and CG concrete decreased with increasing compressive stress σ_1, as indicated in Table 2. The behavior of the tensile strength (*St*) for NG and CG concrete, as calculated using the iterative best-fit procedure, was similar to that of the measured notch tensile strength.

The calculated tension softening diagrams for NG and CG concrete are given in Figure 8 for the compressive loading stages of σ_1/fc = 0.0, 0.30, and 0.60. The results show that the critical crack width of the concrete for σ_1/fc = 0.0 is about 0.15 mm and that for σ_1/fc = 0.6 is more than 0.25 mm. The diagrams also show that the cohesive stress at the lower part of the curve when σ_1/fc = 0.6 is higher than when σ_1/fc = 0.0. Thus, the higher cohesive stress at the lower part of the curve is induced as a result of aggregate

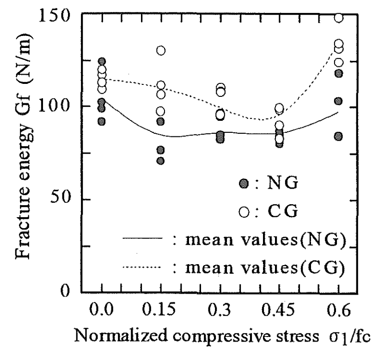

Figure 6. Influence of compressive stress σ_1 on the specific fracture energy *Gf*

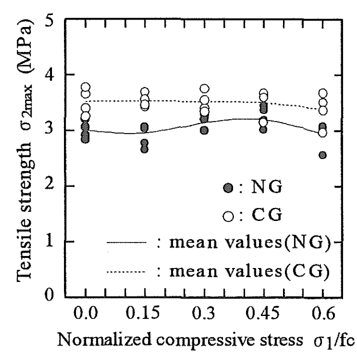

Figure 7. Influence of compressive stress σ_1 on the notch tensile strength σ_{2max}

Table 2. Calculated tensile strength (*St*) and Young's modulus (*Ec*)

σ_1/fc		0.0	0.15	0.30	0.45	0.60
Ec (GPa)	NG	24.3	24.9	23.2	22.2	21.7
	CG	28.2	27.9	28.3	25.1	23.2
St (MPa)	NG	2.46	2.59	2.76	2.85	2.25
	CG	3.30	3.13	2.55	2.42	2.44

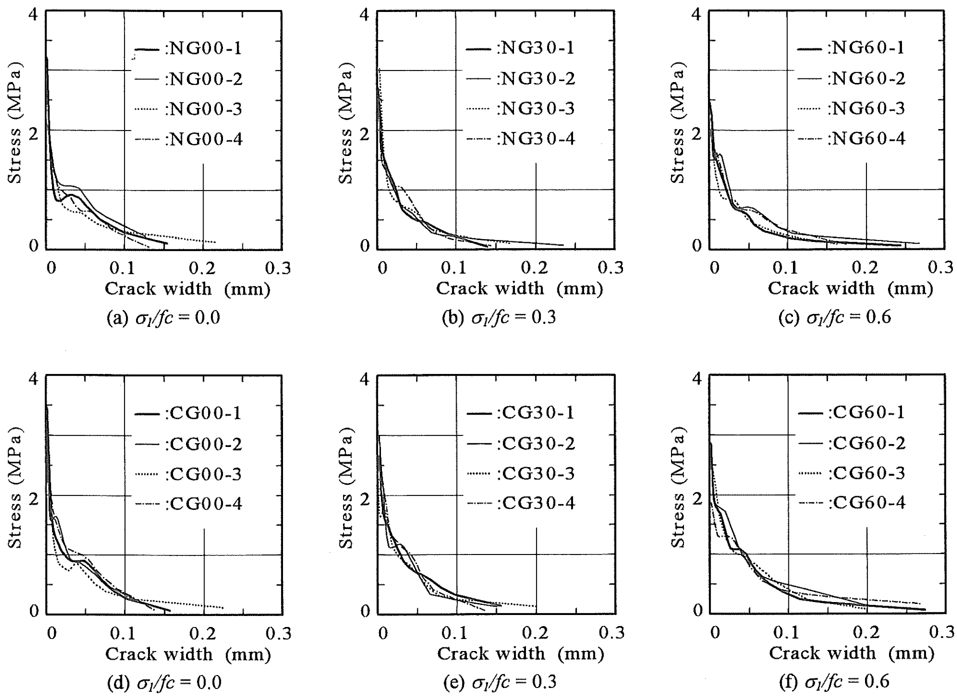

Figure 8. Determined tension softening diagrams

interlock or multiple macro-cracking, as described by Tschegg et al. (1995). This leads to an increase in the fracture energy of the concrete subjected to a compressive stress $\sigma_l/fc = 0.6$.

5 CONCLUSIONS

The fracture properties of concrete under biaxial loading conditions were investigated using the wedge splitting and polylinear inverse analysis methods. Polylinear inverse analysis provided the required tension softening diagrams from the wedge splitting test results. The experimental and analytical results indicate that compressive loading influences both the tension softening properties and the fracture energy of concrete.

6 ACKNOWLEDGMENTS

The author would like to thank Mr. T. Miyamoto for his assistance with the experiments. The author also would like to thank Dr. E. K. Tschegg, Professor of the Institute of Applied and Technical Physics, Technical University, Vienna, for his originality in developing the wedge splitting test methods.

7 REFERENCES

Ishiguro, S. 1997. Tension softening diagrams of concrete under biaxial loading. *Proc. of JCI*, 19(2): 33-38. (in Japanese)

Kitsutaka, Y., Kurihara, N. & Nakamura, S. 1998. Evaluation method of tension softening properties. In Y. Kitsutaka & H. Mihashi (eds), *FRAMCOS-3 Pre-Conference Workshop on Quantitative Evaluation Methods for Toughness and Softening Properties of Concrete, Gifu, Japan*: 46-63.

Nakamura, S., Kitsutaka, Y., Mihashi, H. & Uchida, U. 1999. Discussion on standard evaluation method for tension softening properties of concrete. *Concrete Research and Technology* 10(1): 151-164. (in Japanese)

Tschegg, E.K. 1991. New equipment for fracture tests on concrete. *Material Testing*, 33: 338-343.

Tschegg, E.K., Kreuzer, H. & Zelezny, M. 1992. Fracture in concrete under biaxial loading – Numerical evaluation of wedge splitting test results. In Z.P. Bazant (ed.), *Proc. of the 1st Int. Conf. on Fracture Mechanics of Concrete Structures*, London, Elsevier Applied Science: 455-460.

Tschegg, E.K., Elser, M. & Tschegg-Stanzl, S.E. 1995. Biaxial fracture tests on concrete – development and experience. *Cement and Concrete Composites*, 17: 57-75.

Uchida, Y., Kurihara, N., Rokugo, K. & Koyanagi, W. 1995. Determination of tension softening diagrams of various kinds of concrete by means of numerical analysis. In F.H. Wittmann (ed.), *Proc. of the 2nd Int. Conf. on Fracture Mechanics of Concrete Structures*, Freiburg, Aedificatio: 17-30.